Role of melt during deformation in the deep crust

Cameron Davidson[1], Stefan M. Schmid[1] and Lincoln S. Hollister[2]
[1]*Geologisches Institut der Universität, Bernoullistrasse 32, CH-4056 Basel, Switzerland;* [2]*Department of Geological and Geophysical Sciences, Princeton University, Princeton, New Jersey 08544, USA*

ABSTRACT

Deformation in the deep crust is strongly influenced by the presence of melt. Injected melt (or magma) weakens the crust because strain will tend to localize where melt is present. The amount of strain a pluton may accommodate is dependent on the length of time it takes for a pluton to crystallize and the strain rate. For plutons that intrude into rocks which are near the solidus temperature of the melt, crystallization times can be quite long (> 1Myr).

Partial melting of deep crustal rocks can lead to melt-enhanced embrittlement. This occurs because the volume change for most melting reactions is positive. Therefore, when the rate of melt production outpaces the rate at which melt can leave the system, the melt pressure increases. Eventually, the melt pressure may become sufficiently high that the melting rocks behave in a brittle fashion and fracture. Conjugate sets of dilatant shear fractures filled with melt occur in migmatite from the Central Gneiss belt (Canada); this suggests that melt-enhanced embrittlement occurred in these rocks. An expression which relates the magnitude of differential stress to the angle between conjugate dilatant shear fractures is derived. Assuming that migmatite has a small tensile strength, differential stresses are $\leqslant 20$ MPa in migmatitic rocks at the time melt-enhanced embrittlement occurs. The occurrence of melt-enhanced embrittlement shows that a switch in deformation mechanism from plastic flow to cataclasis is possible in the deep crust during melting. Furthermore, repeated episodes of melt-enhanced embrittlement in migmatitic rocks may be an efficient mechanism for extracting melt from partially melted terrains.

Terra Nova, **6,** 133–142, 1994.

INTRODUCTION

Many recent studies have addressed the close association of deformation and the intrusion of igneous rocks during orogenesis (e.g. Hutton, 1982; Hollister and Crawford, 1986; Davidson *et al.*, 1992; Karlstrom *et al.*, 1993). These studies show that the emplacement of granitoid plutons is not restricted to extensional tectonic settings. Instead, plutons are reported to intrude into a variety of settings including strike slip fault zones (Hutton, 1982) and compressional shear zones (Davidson *et al.*, 1992; Karlstrom *et al.*, 1993). Furthermore, Hollister and Crawford (1986) suggest a possible link between intrusion of granitoids and episodes of rapid uplift in mountain belts ('tectonic surges'), and argue that pluton emplacement helps to weaken the crust and concentrate strain where melt is present.

Another area of recent study is the effect of partial melting on the rheology of rocks. In contrast to the field-oriented studies mentioned above, most of these studies are based on experiments performed in the laboratory (Arzi, 1978; van der Molen and Paterson, 1979; Paquet and Francois, 1980; Cooper and Kohlstedt, 1986; Dell'Angelo and Tullis, 1988). All of these studies show that the strength of rocks decreases with the onset of melting; with dramatic weakening (several orders of magnitude) once the rheological critical melt percentage (RCMP) is attained ($\sim$ 20–30% by volume melt; Arzi, 1978). In addition, many, but not all of these studies show that melting promotes cataclasis. In the experiments by van der Molen and Paterson (1979), cataclastic behaviour is reported in all samples run with different melt percentages (<3 to 21%), with melt-filled microfractures oriented at a low angle, or parallel to σ_1. The ubiquitous cataclastic behaviour observed in these samples is probably due to the relatively low confining pressure (300 MPa) used in the experiments. In the high confining pressure experiments (1500 MPa) performed by Dell'Angelo and Tullis (1988), cataclastic behaviour is also observed, but restricted to high melt percentages (10–15%) and high strain rates (10^{-5} s^{-1}). However, at lower melt percentages and strain rates (10^{-6} s^{-1}), their samples deformed mostly by dislocation creep and/or melt-enhanced diffusion creep (Dell'Angelo and Tullis, 1988). Dell'Angelo and Tullis (1988) suggest that cataclastic behaviour occurred in the high melt percent, high strain rate experiments because the melt could not flow out of the sample fast enough, causing high pore pressures.

All of the aforementioned studies directly address, or have implications for the role of melt (or melting) during deformation in the deep crust. This paper discusses some of the important factors which need to be considered when melt is injected into the deep crust, or produced *in situ*. In the case of injected melt, it is emphasized that the crystallization time of a pluton is the important factor controlling strain partitioning and localization. For *in situ* melting, a natural example from British Columbia (Canada) is presented where melting has promoted brittle behaviour during deformation ('melt-enhanced embrittlement'), and we introduce a conceptual model to explain this behaviour.

INJECTED MELT

There are a number of controlling factors which operate during the intrusion of a pluton which determine the mechanical response of the pluton and surrounding rocks. Perhaps the most important of these are the length of time for crystallization of the pluton, and, if present, the nature of regional deformation occurring at the time of intrusion. For rapidly cooled plutons (crystallization times $\ll$ 1Myr) and rather slow strain rates, there is not enough time for a pluton to accommodate significant strains due to regional deformation while it is partially molten. This is illustrated in Fig. 1, where finite strain is plotted against time. For a 'typical' geological strain rate of 10^{-14} s^{-1} (Pfiffner and Ramsay, 1982), a pluton which takes 500 ka to crystallize may have experienced a strain corresponding to an axial ratio much less than 2 while it is above its solidus. In contrast, a pluton which takes 5 Myr to crystallize may achieve axial ratios of 12 or more before crystallizing. Strain rates faster than 10^{-14} s^{-1} will of course allow substantially larger strains to accumulate during any given crystallization time interval.

Davidson *et. al.* (1992) present a thermal model which they use to calculate the crystallization times of sill-shaped plutons intruded into country rocks at different initial temperatures. They show that crystallization times increase markedly as the initial temperature of the country rocks approaches the solidus temperature of the melt (Fig. 2), and that crystallization times can easily exceed 1 Myr for sill-shaped plutons intruded into the hot, deep crust.

These results have profound implications for the overall rheology of a deforming region in the crust which is intruded by melt. In Fig. 3, melt and rock strengths (given in terms of effective viscosities) are plotted against temperature. Diabase and wet quartzite are used to bracket rock strengths (Table 1) because the strength of most crustal rocks falls within the region defined by these two endmembers (Kirby, 1983). Rock strengths (MPa) are converted to effective viscosities ($Pa s^{-1}$) assuming a strain rate of 1×10^{-14} s^{-1}. Melt viscosities are calculated using the method of Shaw (1972), and melt compositions are taken from McBirney (1984). Granodiorite and diorite bracket most calc-alkaline melt compositions and are common in the deep crust.

It is clear from Fig. 3 that common melts are orders of magnitude weaker than most rocks (note log scale). Magmas (melt+crystals) of course will have higher viscosities than pure melt. However, this effect is expected to be minor at melt percentages above the RCMP. Regardless of the significance or exact location of the RCMP, most workers agree that partially molten rocks are significantly weaker than solid rocks even at melt percentages below the RCMP (Arzi, 1978; van der Molen and Paterson, 1979; Paquet and Francois, 1980; Dell'Angelo and Tullis, 1988). Therefore, plutons which remain above their solidus for long periods of time in deforming regions are expected to accommodate large amounts of strain.

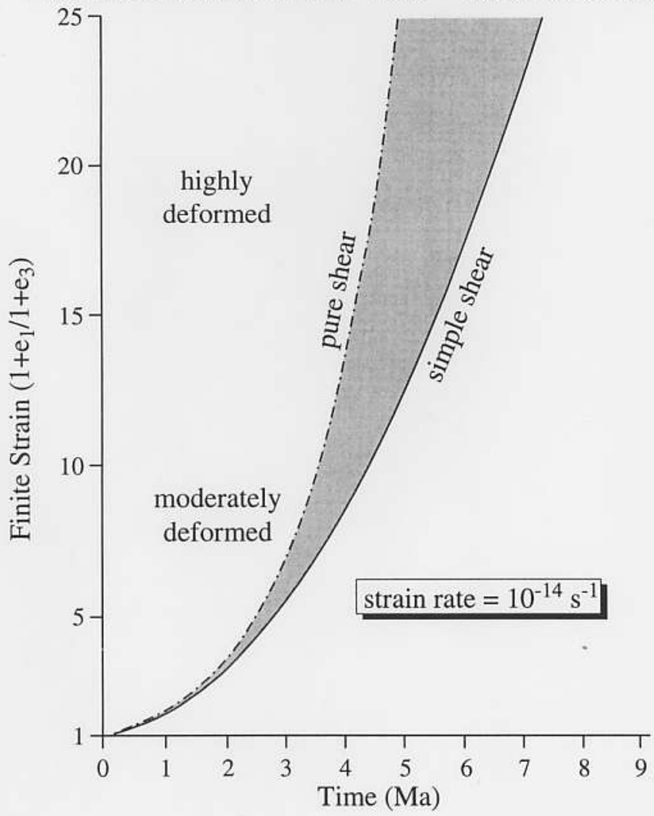

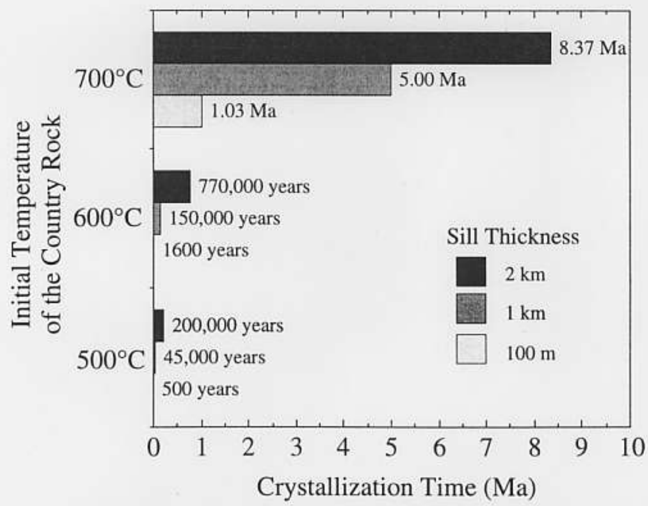

Fig. 1. *(Left) Finite strain vs. time for pure and simple shear (adapted from Pfiffner and Ramsay, 1982).*

Fig. 2. *Crystallization times for sill-shaped plutons of various thickness intruded into country rocks at different initial temperatures (from Davidson* et al.*, 1992).*

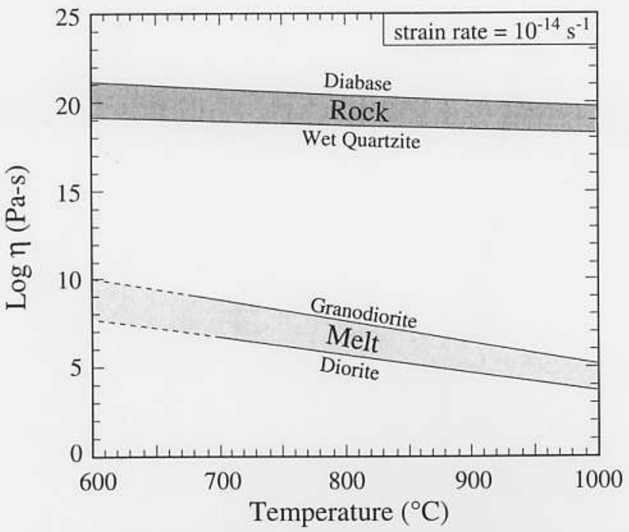

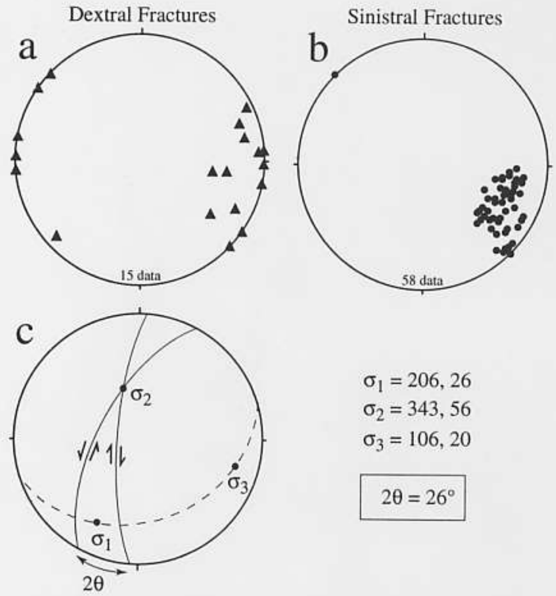

Fig. 3. *(Left) Strength (in terms of effective viscosity) vs. temperature for common rocks and silicate melts. See text for discussion.*
Fig. 5. *(Right) Equal-area lower hemisphere projections of poles to the planes of dilatant shear fractures from the Central Gneiss belt. (a) Fractures with dextral offset. (b) Fractures with sinistral offset. (c) Average orientation of the two sets of fractures (great circles) with sense of offset shown by the arrows. Orientation of the principle stress directions calculated from the average fracture orientations are also shown (orientations at right are given in terms of dip direction, and angle).*

Table 1. Plastic flow constants and tensile strengths used in this paper.

	$\varepsilon = A\Delta\sigma^n \exp(-Q/RT)$				
Rock type	$\log_{10}A$ (GPa^{-n}s^{-1})	n n	Q (kJ mol^{-1})	T_0 (MPa)	Ref.
wet quartzite	3.0	2.6	134	—	Kirby (1983)
diabase	6.5	3.4	260	—	Kirby (1983)
Gosford sandstone	—	—	—	−3.6	Suppe (1985)
Frederick diabase	—	—	—	−40	Suppe (1985)

For the geologist, this is an important fact to appreciate, because much of that strain goes unrecorded due to the generally weak fabric produced during magmatic flow.

IN SITU MELTING

Anatexis of deep crustal rocks is a common feature in orogenic belts, and the petrological consequences of partial melting and formation of migmatites have been addressed by many authors (e.g. Ashworth, 1985). Perhaps less well studied and understood is the effect of anatexis on deformation. Many migmatites show evidence for extremely viscous and mobile behavior and are commonly characterized by somewhat chaotic structures. However, in some migmatite terrains, there are structures present which indicate that these rocks may also behave in a brittle fashion (e.g. Pattison and Harte, 1988; Fig. 4).

The migmatite shown in Fig. 4 is from the Central Gneiss belt of northern British Columbia (Crawford *et al.*, 1987). These rocks were intruded by large volumes of tonalitic magma and experienced anatexis during uplift and exhumation between 60 and 48 Ma (Crawford *et al.*, 1987). Locally within the Central Gneiss belt, melt-filled fractures are present (Fig. 4), which have consistent orientations (Fig. 5), and sometimes occur in conjugate Mohr-type sets (Fig. 4b). In addition to these dilatant shear fractures, ductile shear zones and semi-brittle shear fractures are present. Figure 4c shows a transition from distributed ('ductile') deformation in leucocratic layers, to semi-brittle fractures filled with melt, and finally discrete faulting (with melt filling the fracture) and no strain in adjacent rocks. This clearly points to the simultaneous activity of deformation mechanisms provoking brittle and 'ductile' behaviour within the same outcrop.

The conjugate geometry of these fractures (Fig. 4b), and the observation that melt fills the fractures, suggest that these are dilatant shear fractures which formed while the rocks were partially melted. The discontinuous nature of these melt-filled fractures, and the fact

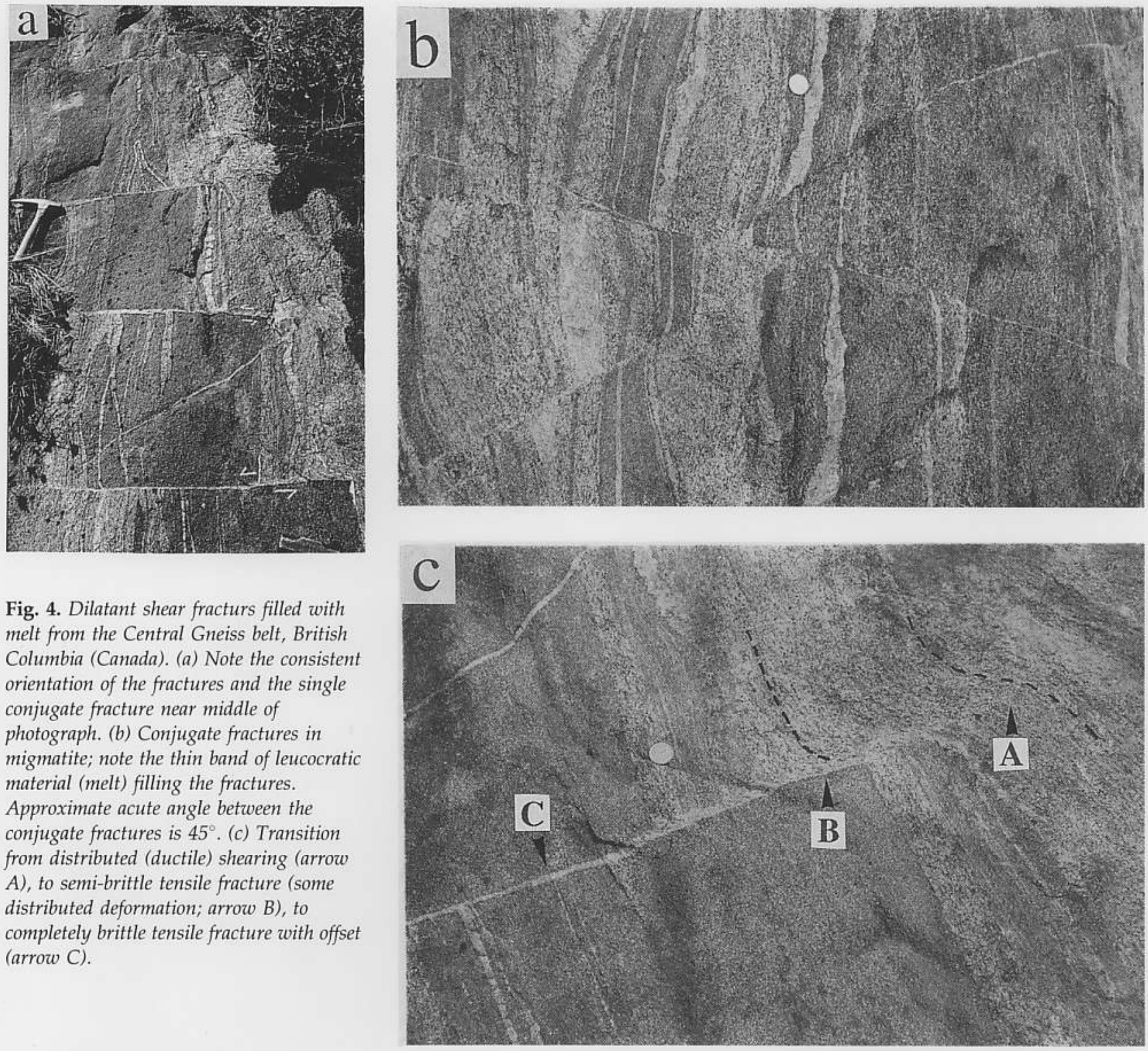

Fig. 4. *Dilatant shear fracturs filled with melt from the Central Gneiss belt, British Columbia (Canada). (a) Note the consistent orientation of the fractures and the single conjugate fracture near middle of photograph. (b) Conjugate fractures in migmatite; note the thin band of leucocratic material (melt) filling the fractures. Approximate acute angle between the conjugate fractures is 45°. (c) Transition from distributed (ductile) shearing (arrow A), to semi-brittle tensile fracture (some distributed deformation; arrow B), to completely brittle tensile fracture with offset (arrow C).*

that the displacements along the fractures die-out into ductile shear zones (Fig. 4c), argue against the melt filling pre-existing fractures. Below, we present a simple conceptual model to explain how these dilatant shear fractures may have formed.

Melt-enhanced embrittlement

The brittle behaviour exhibited by the migmatites from the Central Gneiss belt suggest a possible switch in deformation mechanism from plastic flow to cataclasis during melting; we call this process melt-enhanced embrittlement. The process by which this occurs is analogous to that of hydraulic fracturing used by reservoir engineers in the petroleum industry.

Volume increase upon melting

Most crustal rocks experience about a 10% increase in volume upon wholesale melting (Philpotts, 1990). However, in migmatites, melting is probably not congruent, but rather, is accomplished by incongruent melting forming new solid phases and a melt phase. These melting reactions are predominantly fluid-absent reactions (that is, no free fluid phase is present). This is because any free H_2O-rich fluid will be consumed immediately during the early stages of deep crustal melting due to the high solubility of H_2O in silicate melts at pressure (Burnham, 1979). Furthermore, for typical water contents of deep crustal rocks, fluid-present melting will produce only small amounts of melt (<2 vol.%; Patiño Douce *et al.*, 1990). Once, this fluid-phase is consumed, melting will occur wunder fluid-absent conditions via the breakdown of hydrous phases.

The most common hydrous phases in metapelites are muscovite and/or biotite. Experimental investigations on vapour-absent breakdown of muscovite and biotite in metapelites show

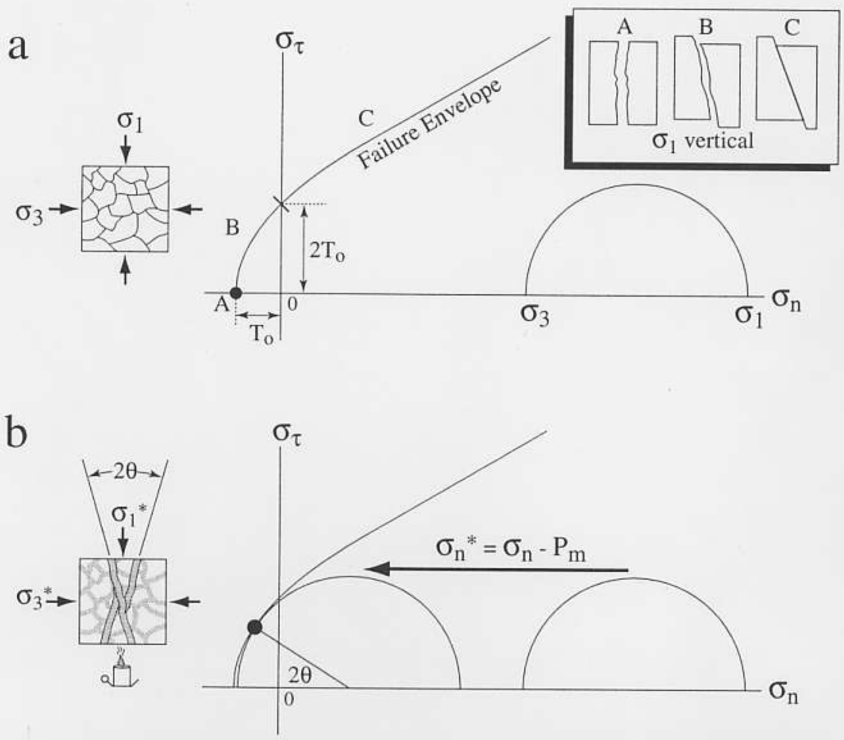

Fig. 6. *Conceptual model for melt-enhanced embrittlement represented on a Mohr-type diagram. The failure envelope is given by Griffith's theory for $\sigma_n < 2T_0$. Tensile fractures oriented parallel to σ_1 form when the Mohr circle touches the failure envelope at A (see inset); dilatant shear fractures form in region B ($\sigma_n < 0$); and compressional shear fractures form in region C. (a) Rock with an imposed differential stress prior to melting which is below that needed for fracture. (b) Upon melting, the melt pressure (P_m) increases and the effective normal stresses are reduced by an amount equal to the melt pressure (law of effective stress, where $\sigma_n{}^*$ = the effective normal stress). Eventually the melt pressure is sufficiently high that the Mohr circle touches the failure envelope, and the partially melted rock fractures. If the Mohr circle touches the failure envelope in region B (see above), then two potential orientations of dilatant shear fractures may form which have an acute angle of 2θ between them.*

that significant melt production (>10%) does not occur until the initiation of biotite breakdown (Vielzeuf and Holloway, 1988; LeBreton and Thompson, 1988). The slopes of these breakdown reactions are steep and positive in P–T space (Le breton and Thompson, 1988), and the change in entropy of the melting reaction (ΔS_r) must be positive (producing a disordered melt phase from crystalline phases); therefore, the volume change of the reaction (ΔV_r) must also be positive ($dP/dT = \Delta S_r / \Delta V_r$). The presence of small-scale folds commonly found in migmatites [similar to those found in hydrated anhydrite (gypsum)] also suggest a positive ΔV_r.

Since the common melt forming reactions have a positive ΔV_r, melting creates a space problem. Therefore, if the rate of melting exceeds the rate at which the melt can escape, the melt pressure (equivalent to the pore-fluid pressure, because the viscosity of melt is very much lower than solids; Fig. 3) will increase dramatically in a given volume of rock with very small percent melting. If this rock unit is under a deviatoric stress ($\Delta\sigma$), then the effective normal stresses will be reduced by an amount equal to the melt pressure (law of effective stress). Eventually, the melt pressure will increase to a point where the rock can no longer support the imposed $\Delta\sigma$, and the rock will fracture (Fig. 6). The mode of fracture depends on where the Mohr circle (diameter = $\Delta\sigma$) touches the fracture envelope as it is translated to the left (Fig. 6a). If a fracture is filled with melt as shown in Fig. 4, then the effective normal stress across the fracture must be tensile, and a tensile (A, Fig. 6a), or dilatant shear fracture will form (region B, Fig. 6a).

State of stress and permeability

In a region undergoing partial melting, one can imagine a complex interplay between rate of melting, melt permeability, state of stress, and strain rate. Because of the high temperatures, deviatoric stresses will be relatively low; that is, at or below the stress needed for plastic flow (crystal-plastic or melt-enhanced diffusion creep). In order for the melt pressure to increase and embrittlement to occur, melt permeability must be sufficiently low that the flow rate of the melt is lower than the rate of melting. Permeability, in turn, is dependent on the geometry of the melt phase with respect to the crystalline phases. The geometry of the melt phase in partially melted rocks is dependent upon a number of factors including melt fraction, wetting angles, and (probably) state of stress (Jurewicz and Watson, 1985).

Partial melting experiments under hydrostatic conditions in granitic systems suggest that for an equilibrium melt fraction (the amount of melt needed to minimize the total surface energy of the system), the melt phase forms an interconnected network of triple junction channels (Jurewicz and Watson 1985; Dell'Angelo and Tullis, 1988). For melt fractions above this amount 2–4%, Jurewicz and Watson, 1985), melt tends to form isolated pools. These results suggest that a finite permeability does exist in partially melted rocks; however, the brittle behaviour seen in the experiments of Dell'Angelo and Tullis (1988), and the natural example from the Central Gneiss belt, suggest that rock permeability to melt must be relatively low in some partially melted rocks, thus allowing the generation of high pore pressures which leads to cataclasis and/or fracture.

State of stress and melt-enhanced embrittlement

The differential stress ($\Delta\sigma$) when melt-enhanced embrittlement occurs can be estimated (in theory) if the shape of the failure envelope (Fig. 6) is known. As will be shown below, the important parameter for determining $\Delta\sigma$ for a dilatant shear fracture is the value of the tensile strength (T_o), or even better, knowledge of the exact shape of the failure envelope in the region where σ_n is tensile (Fig. 6a). Unfortunately, these type of data are difficult to obtain: experimental determinations of T_o for any given rock vary significantly depending on the method used (e.g. table 1-1 in Price and Cosgrove, 1990); and (because of the difficulty) very few experiments have been attempted to try and constrain the shape of the failure envelope in the region where dilatant shear fractures form (Price and Cosgrove, 1990).

Relationship of Δσ and 2θ

The shape of the tensile portion of the failure envelope (σ_n<0) shown in Fig. 6 is given by Griffith's theory and appears to be generally valid for most rocks where $\sigma_1 < |5T_0|$ (Suppe, 1985). The Griffith equation can be rewritten in terms of the principal stresses and T_0:

$$(\sigma_1 - \sigma_3)^2 - 8T_0(\sigma_1 + \sigma_3) = 0, \qquad (1)$$

where $T_0 = |T_0|$, σ_1 and σ_3 are the maximum and minimum (compression positive) stresses, respectively, and $\sigma_1 > -3\sigma_3$ (Paterson, 1978). In addition, Griffith derived an expression which relates the principal stresses and $2\theta'$:

$$\cos(2\theta') = \frac{(\sigma_1 - \sigma_3)}{2(\sigma_1 + \sigma_3)} \qquad (2)$$

where θ' is the angle between σ_1 and the major axis of the elliptical flaw (Paterson, 1978). Implicitly assuming that the crack will spread in its own plane (an assumption made automatically when applying Griffith theory; see discussion in Paterson, 1978), θ' may be equated with θ, the angle between σ_1 and the potential plane of failure (Fig. 6b). Combining equations (1) and (2) and assuming $\theta' = \theta$ gives:

$$(\sigma_1 - \sigma_3) = \frac{4T_0}{\cos(2\theta)}. \qquad (3)$$

This is a useful relationship because the magnitude of the differential stress (in terms of T_0) can be determined from field measurements of dilatant shear fractures. Furthermore, Griffith's theory predicts that 2θ varies from 0° ($\sigma_3 = T_0$) to 45° ($\sigma_n = 0$) in the region where $\sigma_n \leqslant 0$. Therefore, from equation (3) the magnitude of $\Delta\sigma$ is constrained between $4T_0$ and $5.66T_0$. [Price and Cosgrove (1990) arrived at similar limiting values using graphical constructions.]

The acute angle (2θ) between the conjugate fractures shown in Fig. 4b is 45° with an error of about +5° and −3°. (This assumes a ±5° error in dip, and no error in strike as measured in the field). This measured angle suggests that these fractures formed when $\sigma_n \approx 0$, which implies that there should have been little or no opening of the fracture. This is indeed what is observed, where only a thin film of melt is seen along the fractures (Fig. 4b). This suggests that these fractures formed when $\Delta\sigma = 5.66T_0$ ($+0.56T_0$, $-0.28T_0$). If we take the 2θ angle between the average orientation of all the dextral and sinistral melt-filled fractures measured in the field (26°, Fig. 5c), we obtain $\Delta\sigma = 4.45T_0$ (no error estimate made).

In an attempt to place actual numbers on these estimates of $\Delta\sigma$, we use two values of T_0 taken from the literature which define the range of measured T_0 for common rocks: $T_0 = -40$ MPa (Frederick diabase); and $T_0 = -3.6$ MPa (Gosford sandstone) (Table 1). These values of T_0 give $\Delta\sigma = 20.38$ (+2.02, −1.06) MPa and $\Delta\sigma = 226.4$ (+22.4, −11.2) MPa for $2\theta = 45°$, and $\Delta\sigma = 16.02$ MPa and $\Delta\sigma = 178$ MPa for $2\theta = 26°$, for Gosford sandstone and Frederick diabase, respectively. For a tensional shear fracture with $2\theta = 0°$, $\Delta\sigma = 14.4$ MPa for Gosford sandstone, and $\Delta\sigma = 160$ MPa, for Frederick diabase. Therefore, these values of T_0 define a range of $\Delta\sigma$ for the formation of a tensional shear fractures from 14 MPa to 226 MPa (Table 2).

Unfortunately, these estimates of $\Delta\sigma$ are less than satisfactory because they span more than an order of magnitude. Furthermore, differential stresses in excess of 100 MPa seem exceedingly high in view of the low strength expected for migmatite. Gosford sandstone which gives lower estimates $\Delta\sigma$ values (Table 2), is described by Jaeger and Hoskins (1966) as a 'rather weakly cemented quartz sandstone'. Partially melted rocks with an interconnected network of melt filled channels would probably have a similar, or probably lower, tensile strength. Therefore, $\Delta\sigma$ values for the formation of dilatant shear fractures formed during melt-enhanced embrittlement are probably only a few hundred bars ($\leqslant$20 MPa), or lower. This illustrates the following major point; that is, fracturing in migmatites associated with melt-enhanced embrittlement does not require high differential stresses, as might be intuitively expected.

Strain rate, melt pressure, and melt-enhanced embrittlement

Until now, only the formation of brittle fractures has been addressed. However, in the Central Gneiss belt, a range of behaviour from brittle fracture to plastic (ductile) flow along a single 'fracture' (Fig. 4c) was observed. This suggests that melt-enhanced embrittlement occurred contemporaneously with high-temperature plastic flow. If the conceptual model for melt-enhanced embrittlement is correct, then the melt pressure at

Table 2. Calculated differential stresses, strain rates, and melt pressures.

	$\sigma_1-\sigma_3$ (MPa)	ε (wet quartzite) (s^{-1})	ε (diabase) (s^{-1})	λ (P_{melt}/P_{vert})
$2\theta = 0°$				
Gosford sandstone	14.4	9.5×10^{-9}	1.4×10^{-12}	0.99589
Frederick diabase	160.0	5.0×10^{-6}	5.0×10^{-9}	0.95430
$2\theta = 45°$				
Gosford sandstone	20.4	2.4×10^{-8}	4.6×10^{-12}	0.99418
Frederick diabase	226.4	1.2×10^{-5}	1.6×10^{-8}	0.93534

$(\sigma_1 - \sigma_3) = 4T_0/\cos(2\theta)$

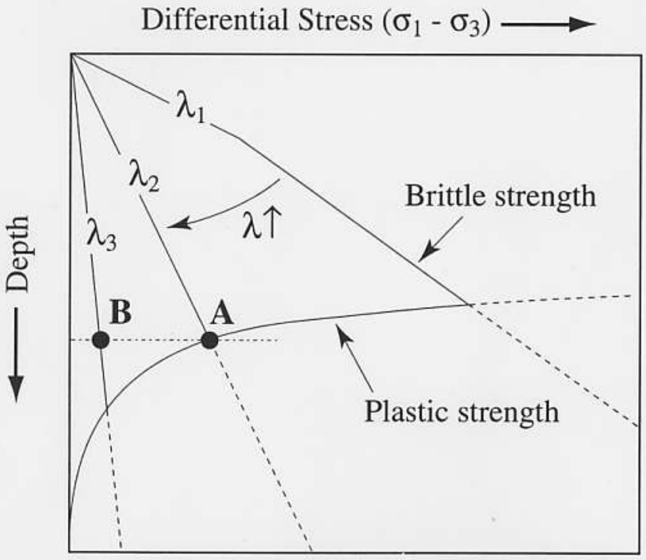

Fig. 7. *Schematic diagram of maximum differential stress vs. depth for the Earth's crust where the upper crust is dominated by brittle behaviour and the lower crust by plastic flow. Differential stresses which occur to the right of the curves are unstable. An increase in pore-fluid pressure (expressed in terms of λ, see text) forces the brittle strength curve to the left. Melt-enhanced embrittlement occurs when partially melted rocks, which are deforming by plastic flow in response to an imposed differential stress at point A, are intersected by the brittle strength curve (λ_2) due to an increase in melt pressure. If the same rocks are under some lower differential stress (not flowing at reasonable strain rates), the higher melt pressures (λ_3) are needed for embrittlement to occur (point B).*

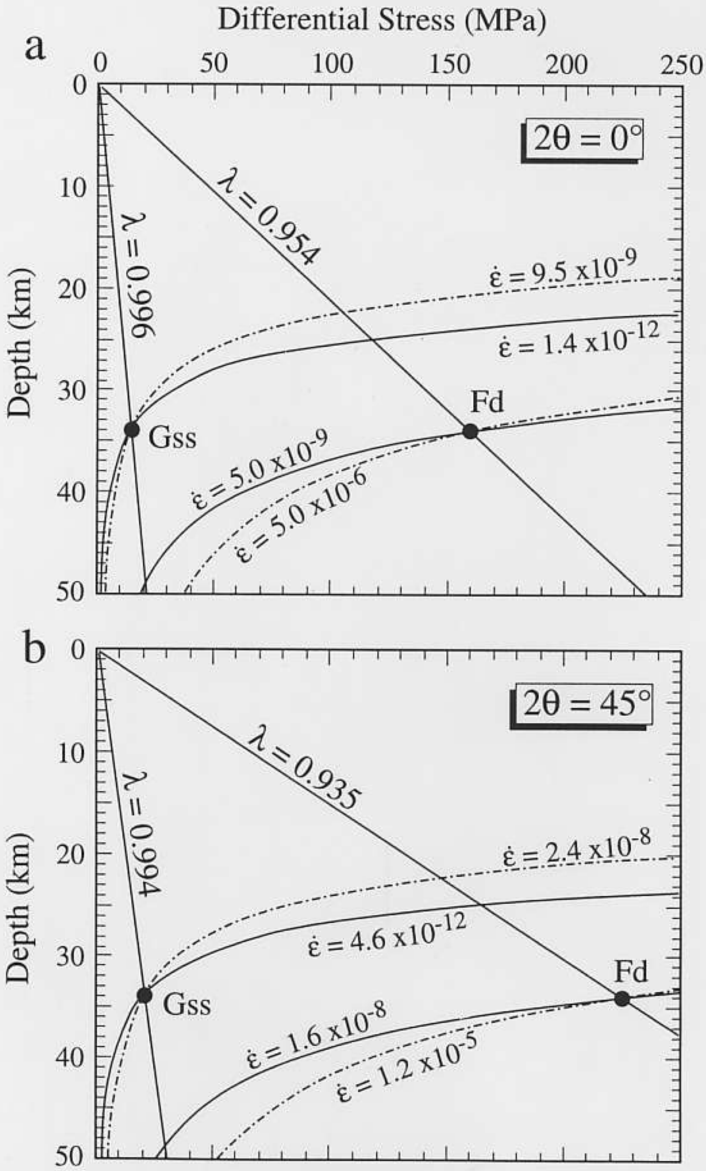

Fig. 8. *(Right) Maximum differential stress vs. depth for the Earth's crust assuming different crustal rheologies. Gss and Fd are rock strengths for Gosford sandstone and Frederick diabase, respectively, calculated from equation (3) for different values of 2θ. Dot-dashed curves are for wet quartzite and solid curves are for diabase rheologies calculated for the strain rate shown (Table 2). λ is calculated so that the brittle curve passes through the desired rock strength. (a) Rock strengths and pore pressures for $2\theta = 0°$. (b) Rock strengths and pore pressures for $2\theta = 45°$. See text for discussion.*

the time of embrittlement will be close to the confining pressure, and the strength of the migmatite will be the same both in respect to brittle fracture and plastic flow. This latter point is visualized in Fig. 7, where deviatoric stress is plotted against depth (see Brace and Kohlstedt, 1980). The 'brittle' and 'plastic' strength curves in Fig. 7 define the deviatoric stress a rock can withstand (its strength) before the onset of deformation associated with brittle behaviour or plastic flow. The maximum strength of the crust occurs at the intersection of these two curves, which is often referred to as the 'brittle-ductile' transition, and which we refer to as the brittle–plastic transition. The position of the brittle curve is mostly dependent on the lithostatic pressure gradient and the fluid pressure. The position and shape of the plastic curve is dependent on composition, strain rate, and the temperature gradient in the crust (Brace and Kohlstedt, 1980).

For a given composition, strain rate, and thermal structure, the depth of the brittle–plastic transition is solely dependent on the pore-fluid pressure. If the pore pressure is hydrostatic ($\lambda \approx 0.37$ where $\lambda = P_f/P_{lith}$, and where P_f is fluid pressure and P_{lith} is lithostatic load), then the brittle–plastic transition in a quartz-dominated crust occurs between 10 km and 16 km ($dT/dz = 15°C\ km^{-1}$ and $25°C\ km^{-1}$). Increasing the pore pressure above hydrostatic increases the depth of the brittle-plastic transition (Fig. 7), and at very high pore pressures (as $\lambda \to 1$), brittle fracture may occur at any depth. If the fluid phase is a silicate melt rather than an aqueous fluid, λ will tend to be close to 1 because of the higher densities of melts (about 2.4 g cm^{-3} for silicic melts; Lange and Carmichael, 1990). Of course it is unrealistic to expect an interconnected network of melt to exist all the way to the surface; however, for now it is a conceptual convenience to assume that $P_m = \rho g h$ (P_m is melt pressure, ρ is density of the melt, g is acceleration due to gravity, and h is depth), so that we may visualize how melt-enhanced embrittlement works (Fig. 7, and see below).

For the case of partial melting and melt-enhanced embrittlement, one can imagine a situation where deep crustal rocks are at their melting temperature, and are flowing in response to an imposed $\Delta\sigma$ (point A, Fig. 7). Initially these rocks deform by plastic flow because point A is situated below the critical stress needed for brittle deformation (λ_1, Fig. 7). As these rocks melt, λ begins to increase and the brittle strength curve in Fig. 7 moves to the left. Eventually, λ becomes sufficiently high (λ_2, Fig. 7) that brittle strength equals plastic strength (point A, Fig. 7) and the migmatite may fracture or flow contemporaneously, as observed in Fig. 4c. Alternatively, $\Delta\sigma$ may be less than the deviatoric stress needed for plastic flow at reasonable strain rates (point B, Fig. 7). In such a case, λ needs to be even higher (λ_3, Fig. 7) to promote fracture. For the first case (point A, Fig. 7), an estimate of the local strain rate and melt pressure can (in theory) be calculated from the magnitude of the differential stress (determined from equation 3) if, at the time of embrittlement, the depth at which embrittlement took place, the temperature profile, and the appropriate rock properties for the crust are known.

In practice, most of these variables are too poorly constrained to make any kind of meaningful estimate; however, it is instructive to look at a general case, using a given temperature profile, depth, the values of $\Delta\sigma$ determined previously, and extreme values for the flow laws (Fig. 8). Figure 8 is constructed using Byerlee's law ($\Delta\sigma = 3.9\sigma_3^*$; $\sigma_3 < 120$ MPa) for the brittle portion of the curves assuming that σ_1 is horizontal and $\sigma_3^* = \rho g h(1-\lambda)$ (Kirby, 1983). Note that the strength of brittley deformed rocks is approximated with frictional strength following a procedure used by most authors when discussing rock strength as a function of depth and pore pressure (e.g. Brace and Kohlstedt, 1980; Molnar, 1992). This approximation is considered reasonable because problems such as fracture propagation and mechanisms of failure are not addressed (see Spence and Turcotte, 1985; Rubin, 1993). The plastic curves are calculated using the same flow law data used in Fig. 3 (Table 1) for different strain rates. A geothermal gradient of 25°C km^{-1} is used, which gives 850°C (approximately the temperature for biotite breakdown and significant melting in fluid-absent pelitic rocks; see previous sections) at a depth of 34 km. For a given magnitude of $\Delta\sigma$, values of λ and strain rate are adjusted until the brittle, wet quartzite, and diabase curves intersect at 34 km depth.

The calculated strain rates from the above exercise (Table 2) range over many orders of magnitude (10^{-5}–10^{-12} s^{-1}). It is interesting to note that all of the calculated rates are substantially faster than those quoted in the literature as 'typical' (10^{-13}–10^{-15} s^{-1}; e.g. Pfiffner and Ramsay, 1982). Strain rates calculated using the tensile strength of Gosford sandstone range from 10^{-8} to 10^{-12} s^{-1}. However, for lower values of T_0 (as expected for migmatite), strain rates will be slower. In order to obtain a strain rate of 10^{-14} s^{-1}, T_0 values of $\sim$ 0.01–0.8 MPa are needed. Such low T_0 values cannot be excluded in the case of partially molten rocks.

While strain rate estimates heavily depend on the (difficult to estimate) T_0 values, the values of λ are consistently high (>0.9). This is to be expected at great depths where brittle behaviour can only successfully compete with plasttic flow if brittle strength is very low (that is, λ very high). While constant λ values were only chosen as a conceptual convenience in constructing Figs 7 and 8, high melt pressures are expected to build-up locally (and temporarily) due to the volume increase during partial melting if the permeability of the partially molten rock is low. In addition, note that lower values of T_0 yield higher values of λ; therefore, melt-enhanced embrittlement in migmatite may imply extremely high melt pressures (λ>0.99). Of course, if melt-enhanced embrittlement occurs at shallower levels in the crust, then λ will be somewhat lower (for the same $\Delta\sigma$); however, not significantly lower, because of the high temperature gradient needed to promote melting. (A higher temperature gradient simply shifts the plastic curves to shallower levels).

CONCLUSIONS

The presence of melt in the deep crust has important implications for the deformational behaviour of deep crustal rocks. Since the strength contrast is significant between rock and melt (Fig. 3), melt (or magma) injected into deep crustal rocks weakens the crust locally, and strain is temporarily concentrated where melt is present. The length of time for crystallization of a pluton is the important factor in determining how much of an effect pluton emplacement will have on strain localization. If a pluton intrudes into rocks which are at temperatures near the solidus temperature of the melt, then the pluton may remain above its solidus for long periods of time (>1 Myr; Fig. 2). Large amounts of strain in a pluton may go unrecorded if one considers the amount of strain a partially molten pluton could accommodate over a few million years under 'normal' strain rates (Fig. 1), and if the fabric produced by magmatic flow is weak, as commonly observed. However, weak magmatic fabrics are sometimes associated with deformed enclaves which demonstrate large strains and are consistent with the solid state strains observed in the surrounding rocks due to regional deformation (Davidson *et al.*, 1992; Vogler and Voll, 1981).

Partial melting of deep crustal rocks is another important process which occurs during orogenesis. During partial melting, a space problem arises due to the positive volume change of melting. If the rate of melt production outpaces the rate at which melt can escape from the system, the melt pressure (pore-fluid pressure) will increase rapidly. Eventually, the melt pressure may become sufficiently high that the melting rocks behave in a brittle fashion and fracture (Figs 4 and 6). This process is called melt-enhanced embrittlement.

The differential stress at the time melt-enhanced embrittlement occurred can be estimated from conjugate sets of dilatant shear fractures if one assumes that dilatant shear fractures follow Griffith's law of failure, and that the tensile strength of the rock is known (3). Conversely, (3) can be used to calculate the tensile strength of rock if the magnitude of $\Delta\sigma$ is somehow known or can be estimated. In view of the low differential stresses expected to prevail in migmatite terranes, the tensile strength of partially melted rock must be very low (similar to, or less than that of Gosford sandstone). The major point emerging from our simple calculation is that embrittlement does not require high differential stresses in migmatitic rocks ($\leqslant$20 MPa).

Melt-enhanced embrittlement may act to further weaken rocks to very low differential stresses (below $\Delta\sigma$ needed for plastic flow; pt. B, Fig. 7); or, may occur while the rocks are flowing plastically in response to an imposed $\Delta\sigma$ (pt. A, Fig. 7). The latter situation is common in partially melted terrains under compression, and is of some interest because strain rates and melt pressures can be estimated (in theory) if dilatant shear fractures form (Fig. 8). The strain rate calculations depend heavily on the values used for the tensile strength. Strain rates of 10^{-13} to 10^{-14} s^{-1}, as commonly quoted in the literature, require very low tensile strengths (0.01–1.7 MPa). However, strain rates faster than 'normal' are expected in major crustal shear zones. Hence, we are not forced to assume extremely low T_0 values a priori. Calculated melt pressures, on the other hand, are ubiquitously high ($\lambda > 0.9$) regardless of the rock properties chosen. In addition, for rocks with very low tensile strength, extremely high melt pressures ($\lambda > 0.99$) are needed for embrittlement to occur. This implies that very low permeabilities are possible in partially molten rocks as in our field example (Fig. 4).

To conclude, melt-enhanced embrittlement does occur in the dep crust as evidenced by migmatites from the Central Gneiss belt (Fig. 4). This shows that a switch in deformation mechanism from plastic flow to cataclasis is possible in the deep crust during melting. However, preservation of structures which indicate that melt-enhanced embrittlement occurred is probably rare because of subsequent elimination of these structures by plastic flow. In our example from the Central Gneiss belt (Fig. 4), the local differential stress at the time of embrittlement was probably below that needed for plastic flow. Subsequent uplift and erosion effectively quenched the rocks and preserved the dilatant shear fractures. For the more common case, where plastic flow eliminates these fractures with time, a scenario can be envisioned where plastic flow of partially melted rocks is punctuated by episodes of melt-enhanced embrittlement. After each event, the melt pressure will drop as the melt drains from the system along the newly formed fractures, followed by a rise in melt pressure until the next event. This episodic nature of melt-extraction may offer a convenient way to extract melt from partially melted terrains, and may be partially responsible for the chaotic structures often observed in migmatites.

ACKNOWLEDGEMENTS

Support from Schweizerischer Nationalfonds grants 21-29804.90 and 20-35891.92 is gratefully acknowledged. We thank E. Rutter and an anonymous reviewer for detailed and constructive comments which helped improve the content. Many thanks to Niko Froitzheim, Reto Gieré, Renée Heilbronner, Holger Stünitz, and Mathias Hafner for discussions which helped clarify the subject matter. C. Davidson also wishes to acknowledge Neil Mancktelow, who pointed out that migmatites will be strongest when melt-enhanced embrittlement and plastic flow occur contemporaneously.

REFERENCES

Arzi A.A. (1978) Critical phenomena in the rheology of partially melted rocks, *Tectonophys.*, **44**, 173–184.

Ashworth, J.R. (1985) *Migmatites*. Blackie, Glasgow, 302 pp.

Brace W.F. and Kohlstedt D.L. (1980) Limits on lithospheric stress imposed by laboratory experiments, *J. geophys. Res.*, **85**, 6248–6252.

Burnham C.W. (1979) The importance of volatile constituents. In: *The Evolution of the Igneous Rocks* (ed. by H.S. Yoder, Jr.), pp. 439–482. Princeton University Press, New Jersey.

Copper R.F. and Kohlstedt D.L. (1986) Rheology and structure of olivine-basalt partial melts, *J. geophys. Res.*, **91**, 9315–9323.

Crawford M.L., Hollister L.S. and Woodsworth G.J. (1987) Crustal deformation and regional metamorphism across a terrane boundary, Coast Plutonic Complex, British Columbia, *Tectonics*, **6**, 343–361.

Davidson C., Hollister L.S. and Schmid S.M. (1992) Role of melt in the formation of a deep-crustal compressive shear zone: the Maclaren Glacier metamorphic belt, south central Alaska, *Tectonics*, **11**, 348–359.

Dell'Angelo L.N. and Tullis J. (1988) Experimental deformation of partially melted granitic aggregates, *J. Met. Geol.*, **6**, 495–515.

Hollister L.S. and Crawford M.A. (1986) Melt-enhanced deformation: a major tectonic process, *Geology*, **14**, 558–561.

Hutton D.H.W. (1982) A tectonic model for the emplacement of the Main Donegal granite, NW Ireland, *J. Geol. Soc. London*, **139**, 615–631.

Jaeger J.C. and Hoskins E.R. (1966) Rock failure under the Confined Brazilian Test, *J. geophys. Res.*, **71**, 2651–2659.

Jurewicz S.R. and Watson E.B. (1985) The distribution of partial melt in a granitic system: The application of liquid phase sintering theory, *Geochim. Cosmochim. Acta*, **49**, 1109–1121.

Karlstrom, K.E., Miller, C.F., Kingsbury, J.A., and Wooden, J.L. (1993) Pluton emplacement along an active ductile thrust zone, Piute Mountains, southeastern California: Interaction between deformational and solidification processes, *Bull. geol. Soc. Am.* **105**, 213–230.

Kirby, S.H. (1983) Rheology of the lithosphere, *Rev. Geophys. Space Phys.*, **21**, 1458–1487.

Lange, R.L. and Carmichael, I.S.E. (1990) Thermodynamic properties of silicate liquids with emphasis on density, thermal expansion, and compressibility. In: *Modern Methods of Igneous Petrology: Understanding Magmatic Processes* (ed. by J. Nicholls and J.K. Russell). *Rev. Mineral.*, **24**, 25–64.

Le Breton N. and Thompson A.B. (1988) Fluid-absent (dehydration) melting of biotite in metapelites in the early stages of crustal anatexis, *Contr. Miner. Petrol.*, **99**, 226–237.

McBirney A.R. (1984) *Igneous Petrology*. Freeman, Cooper & Company, San Francisco, 504 pp.

van der Molen I. and Paterson M.S. (1979) Experimental deformation of partially-melted granite, *Contr. Miner. Petrol.*, **70**, 299–318.

Molnar, P. (1992) Brace-goetze strength profiles, the partitioning of strike-slip and thrust faulting at zones of oblique convergence, and the stress-heat flow paradox of the San Andreas fault. In: *Fault Mechanics and Transport Properties of Rocks* (ed. by B. Evans and T-F Wong), pp. 435-459. Academic Press, London.

Paquet J. and François P. (1980) Experimental deformation of partially melted granitic rocks at 600–900°C and 250 MPa confining pressure, *Tectonophys.*, **68,** 131–146.

Paterson M.S. (1978) *Experimental Rock Deformation: The Brittle Field.* Springer Verlag, Berlin, 254 pp.

Patiño Douce A.E. (1990) Anatexis and metamprphism in tectonically thickened continental crust exemplified by the Sevier hinterland, western North America, *Earth Planet. Sci. Lett.*, **97,** 290–315.

Pfiffner O.A. and Ramsay J.G. (1982) Constraints on geological strain rates: Arguments from finite strain states of naturally deformed rocks, *J. geophys. Res.*, **87,** 311–321.

Philpotts A.R. (1990) *Principles of Igneous and Metamorphic Petrology.* Prentice Hall, Englewood Cliffs, New Jersey, 498 pp.

Price N.J. and Cosgrove J.W. (1990) *Analysis of Geologic Structures.* Cambridge University Press, 498 pp.

Rubin, A.M. (1993) Tensile fracture of rock at high confining pressure: implications for dike propagation, *J. geophys. Res.*, **98,** 15,919–15,935.

Shaw H.R. (1972) Viscosities of magmatic silicate liquids: an empirical method of prediction, *Am. J. Sci.*, **272,** 870–893.

Spence, D.A. and Turcotte, D.L. (1985) Magma-driven propagation of cracks, *J. geophys. Res.*, **90,** 575–580.

Suppe J. (1985) *Principles of Structural Geology.* Prentice Hall, Englewood Cliffs, New Jersey, 537 pp.

Vielzeuf D. and Holloway J.R. (1988) Experimental determination of the fluid-absent melting relations in the pelitic system, *Contr. Miner. Petrol.*, **98,** 257–276.

Vogler W.S. and Voll G. (1981) Deformation and metamorphism at the south-margin of the Alps, East of Bellinzona, Switzerland, *Geol. Rndsch.*, **70,** 1232–1262.

Manuscript received 31 August 1993; revision accepted 15 December 1993